THE JOURNAL OF PHYSICAL CHEMISTRY C

Article

Cite This: J. Phys. Chem. C 2018, 122, 23230−23241

pubs.acs.org/JPCC

On the Rational Design of Zeolite Clusters for Converging Reaction Barriers: Quantum Study of Aldol Kinetics Confined in HZSM-5

Angela N. Migues,[†,§,#] Qinfang Sun,[†,#] S. Vaitheeswaran,[†,∥] Woody Sherman,[⊥] and Scott M. Auerbach*[,†,‡]

[†]Department of Chemistry and [‡]Department of Chemical Engineering, University of Massachusetts, Amherst, Massachusetts 01003, United States

[§]Department of Chemistry, Stony Brook University, Stony Brook, New York 11794, United States

[∥]Department of Physics and Earth Sciences, Framingham State University, Framingham, Massachusetts 01701, United States

[⊥]Silicon Therapeutics, 300 A Street, Boston, Massachusetts 02210, United States

Supporting Information

ABSTRACT: We have performed density functional theory calculations to investigate the convergence of reaction barriers with respect to zeolite cluster size, for multistep reactions catalyzed in HZSM-5. We constructed cluster models of HZSM-5 using the delta-cluster approach reported previously by us. We then computed barriers for different reaction types to determine the cluster sizes and neighbor-list radii needed to fully treat zeolite confinement effects. In particular, we studied the acid-zeolite-catalyzed aldol reactions of acetone with formaldehyde, furfural, and hydroxymethyl-furfural, in three steps: keto/enol tautomerization of acetone, combination between each aldehyde and the enol, and aldol dehydration. We found that the delta-cluster radius of 4.0 Å consistently converges barriers with respect to cluster size, yielding complete treatments of confinement in HZSM-5 with clusters containing up to 99 atoms. For comparison, periodic density functional theory (DFT) on HZSM-5 includes 288 atoms, requiring 19 times more CPU time in head-to-head comparisons. Our converged acetone−formaldehyde dehydration barrier agrees quantitatively with a comparable barrier obtained with periodic DFT, showing that cluster calculations can converge properties at a fraction of the cost of periodic DFT. Interestingly, we found that the bulkier, furan-containing aldehydes exhibit faster reactivity because of charge delocalization from aromatic rings, which significantly speeds up aldol dehydration.

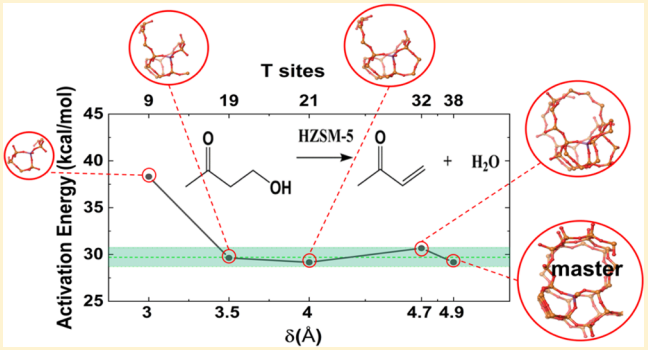

1. INTRODUCTION

Zeolites are the most used catalysts by weight on planet earth because of their regular arrays of stable nanopores with well-defined active sites.[1,2] Discovering the physical chemistry underlying shape-selective zeolite catalysis requires computational methods that accurately and efficiently provide activation energies for complex reactions in confining zeolite pores.[1,2] Broadly speaking, two methods have been applied to computational zeolite catalysis: quantum cluster calculations and periodic planewave methods. Although periodic methods treat long-range forces and zeolite confinement, they may include atoms that do not participate in the chemistry, thereby making the calculations more computationally expensive than necessary.[3] Cluster calculations can reduce computational expense while also providing accurate energetics without explicit inclusion of long-range forces, as we and others have shown in several publications.[4−6] That is because in computing an energy difference such as a barrier for a reaction in a zeolite, the contributions from long-range forces approximately cancel because these are relatively slowly varying interactions, making cluster calculations a practical approach. However, for cluster calculations to be predictive, one must converge barriers with respect to cluster size for each different system studied, which can be tedious. In a previous article,[5] we introduced the "delta-cluster" method, which confines molecules in tailored clusters using a systematic and automated approach involving a single neighbor-list radius, and we demonstrated its power for computing thermodynamic reaction energies for a range of processes in zeolites. In the present article, we apply the delta-cluster method to compute kinetic barriers for reactions in zeolites, using the aldol reaction in zeolites as an important and challenging platform for testing the delta-cluster approach.

We developed the delta-cluster approach to automatically construct zeolite clusters that provide comprehensive treatments of confinement. This is achieved by using the coordinates of adsorbed guest reactant and product geometries

Received: September 5, 2018
Revised: September 12, 2018
Published: September 14, 2018

DOI: 10.1021/acs.jpcc.8b08684
J. Phys. Chem. C 2018, 122, 23230−23241

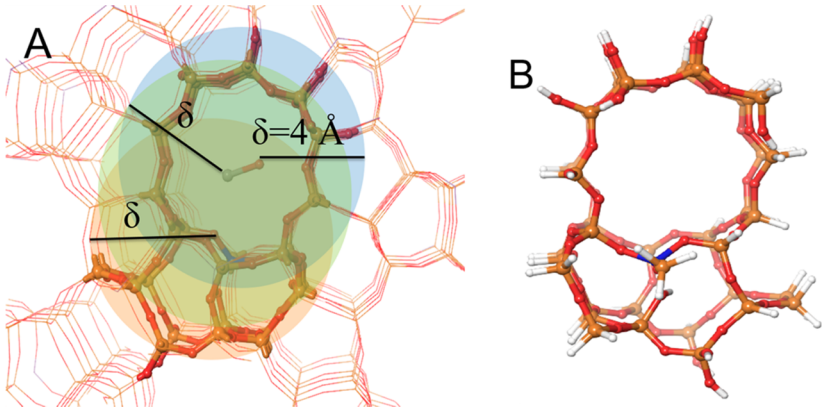

Figure 1. (A) Illustrated scheme for constructing delta cluster of HZSM-5 where carbon monoxide (CO) is used as an example guest molecule. The three spheres centered on guest C, guest O, and zeolite acid site O (all with the same radius, δ = 4.0 Å) are represented by different colors. The union set of the three spheres, plus four required connecting atoms (see text), yields the resulting delta cluster shown in (B), where CO has been removed for clarity and dangling bonds have been capped with hydrogens.

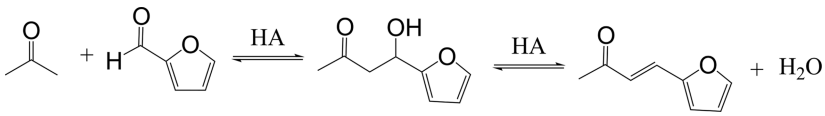

Figure 2. Acid-catalyzed aldol coupling between acetone and furfural (hyaluronic acid is a general acid catalyst), followed by dehydration to generate enone and water.

to identify all zeolite atoms that fall within a collection of spheres (with a given radius δ) centered on all reactant, product, and active-site atoms (please see Figure 1).[5] The motivations for the delta-cluster approach are computational accuracy and efficiency: including the fewest number of atoms necessary to produce comprehensive treatments of confinement and thus accurate energetics, and avoiding cluster convergence tests for each new system and reaction studied. One way to avoid cluster convergence tests is to include the full zeolite unit cell as was done, for example, by Liu et al. in their study of HZSM-5, which included all 96 SiO_2 units (288 atoms) of the MFI unit cell.[3] Such calculations provide a useful benchmark but likely include nonessential atoms, as suggested by cluster convergence studies that produced accurate energetics in HZSM-5 with only about 1/3 of the unit cell.[4] However, the aforementioned study required manual generation of the reduced zeolite systems, which is time consuming, error prone, and not systematic. As such, a reliable, systematic, and automated method for rationally designing converged zeolite clusters remains an important computational tool.

Our study of systematic cluster convergence was also motivated by the observation in our earlier work[4] that relatively large zeolite clusters—presumably large enough to confine guest molecules—can produce very different activation energies, raising the question of whether there is a way to design, a priori, an optimal and converged zeolite cluster for a given reaction. An intuitive way to design clusters of network solids like zeolites is to include atoms some number of bonds away from a central active-site atom (e.g., aluminum at the zeolite Brønsted site). For example, a cluster containing all atoms three bonds from a central atom would be denoted a three-bond cluster. However, we have shown in our previous work[5] on computing thermodynamic reaction energies in zeolites that such a "bond counting" approach suffers from two problems: (i) for a given reaction, clusters obtained from bond counting were found to be consistently larger than delta clusters for the same level of convergence; and (ii) the bond-counting approach offered no single convergence criterion, with some reaction energies converging with four-bond clusters and others requiring seven-bond clusters, while converged delta clusters of different sizes for different reactions were found to be consistent with a single convergence criterion of δ = 4.0 Å. The success of the delta-cluster approach likely stems from tailoring clusters to envelop a given set of adsorbed reactants and products, while the bond-counting approach simply enlarges zeolite clusters without any reference to guest molecule's size or shape. However, it remains to be seen whether delta-cluster convergence of several different reaction barriers can be obtained with a single value of δ. Here, we investigate this issue below using aldol chemistry in HZSM-5 zeolite as an important and challenging platform system, which we now discuss.

The aldol condensation reaction typically joins a ketone to an aldehyde (see Figure 2)[7] and derives its current industrial importance as a primary strategy for upgrading biomass-derived molecules into precursors of biofuels.[8,9] Studying the physical chemistry of aldol condensation—its pathways and energetics—is technologically important for maximizing yields of biofuels while limiting byproducts from further aldol condensation that can clog zeolite pores.[7,9−11] Modeling aldol chemistry in zeolites presents a challenging test of the delta-cluster method for the following reasons: (i) the aldol reaction is a multistep process with three or more steps (depending on the precise pathway); (ii) both unimolecular and bimolecular steps are required; and (iii) industrially relevant aldehydes are bulky with aromatic side groups, requiring accurate treatments of zeolite confinement. Below we study the aldol condensation in HZSM-5 zeolite of acetone with the following aldehydes: formaldehyde, the smallest aldehyde for benchmarking purposes; furfural, the smallest aromatic aldehyde; and hydroxymethyl-furfural (HMF), the

DOI: 10.1021/acs.jpcc.8b08684
J. Phys. Chem. C 2018, 122, 23230−23241

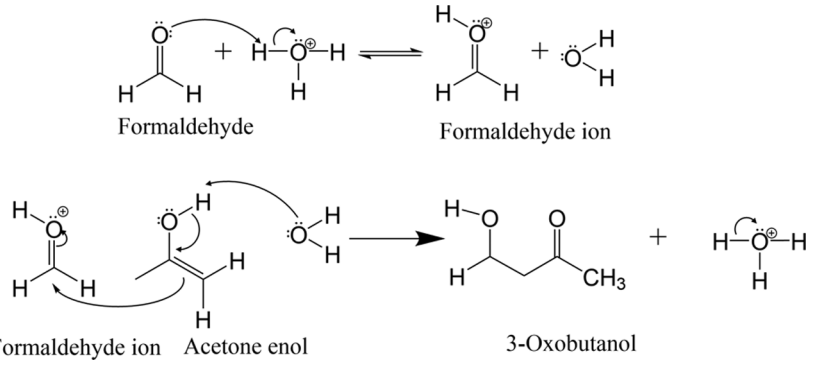

Figure 3. Conventional stepwise mechanism for homogeneous acid-catalyzed bimolecular combination between formaldehyde and acetone enol, involving (i) protonation of formaldehyde and (ii) attack by the acetone enol.

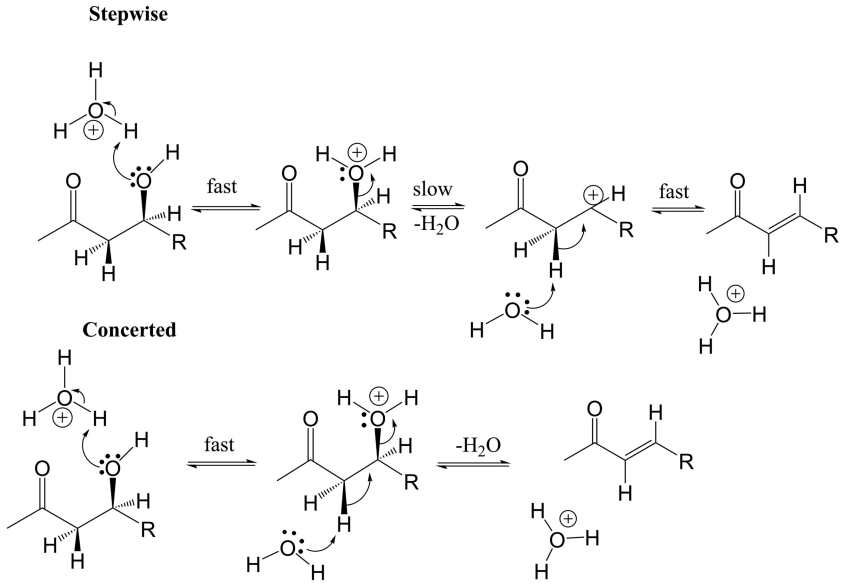

Figure 4. Homogeneous acid-catalyzed aldol dehydration with two different mechanisms: "stepwise" acid-catalyzed dehydration via unimolecular elimination (E1) of water; or "concerted" acid-catalyzed dehydration via bimolecular elimination (E2).

most industrially important biomass-derived aldehyde.[8,12] By studying acetone reacting with aldehydes of increasing size, we aim to answer two important questions: How does the optimal cluster size required to model confinement in zeolites vary with reactant size? And how does reactant bulkiness modulate the rate-determining step of aldol condensation in confining zeolite nanopores? The delta-cluster method helps answer both of these questions.

Under homogeneous acid [e.g., $H_2SO_4(aq)$] catalytic conditions, aldol condensation occurs in three main steps: (i) keto/enol tautomerization (in two elementary steps), (ii) bimolecular combination between the enol and the aldehyde (in three elementary steps; see Figure 3), and (iii) elimination of water to form the olefinic product (in two or three elementary steps; see Figure 4),[11] with the keto/enol reaction thought to be the rate-determining step because of the relative instability of the enol.[13] Several density functional theory (DFT) studies have been reported on aldol chemistry in acidic zeolites to reveal how the aldol mechanism changes upon confinement in nanopores. Boekfa et al.[14] studied the keto/enol tautomerization of acetone in quantum cluster models of HFER, HZSM-5, and HMCM-22 zeolites with the M06-2X density functional. They used clusters of size 34T, where T = Si or Al tetrahedral atoms, and found concerted keto/enol processes with activation energies of 24.9, 20.5, and 16.6 kcal/mol in H-FER, HZSM-5, and H-MCM-22, respectively, decreasing with increasing pore size. In our previous work on the aldol condensation between acetone and formaldehyde in clusters of HZSM-5 and HY zeolites,[4] we studied keto/enol and bimolecular combination steps and found both processes to be concerted in both zeolites. We determined through cluster-size convergence studies that the acetone keto/enol barrier is 20 kcal/mol in both HY (large pore) and HZSM-5 (medium pore) zeolites at the B3LYP+D3 level, in quantitative agreement with Boekfa et al. for HZSM-5, but disagreeing with the trend of decreasing barrier with increasing pore size. We also found very small bimolecular combination barriers (≤2 kcal/mol) in both zeolites, suggesting that the keto/enol reaction is much slower and possibly the rate-determining step of acetone−formaldehyde aldol condensation in HZSM-5.

Liu et al.[3] reported planewave DFT calculations with the Perdew−Burke−Ernzerhof (PBE) density functional on a full unit cell of HZSM-5 to model the self-aldol condensation of acetaldehyde, along with furan−furan and furan−acetaldehyde coupling reactions, considering all steps including the final dehydration step. Liu et al. found a concerted keto/enol process with a barrier for acetaldehyde of 20 kcal/mol and a very small (<2 kcal/mol) bimolecular combination barrier—

DOI: 10.1021/acs.jpcc.8b08684
J. Phys. Chem. C 2018, 122, 23230−23241

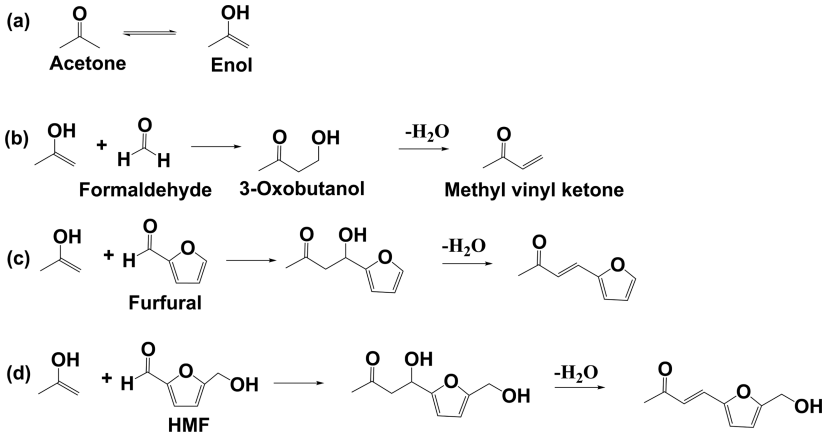

Figure 5. Reactions under study: (a) keto/enol tautomerization of acetone; bimolecular combinations and dehydration between acetone enol and (b) formaldehyde, (c) furfural, and (d) HMF.

consistent with previous quantum cluster results for the acetone–formaldehyde system.[14,4] Liu et al. also found a dehydration barrier for the acetaldehyde self-aldol reaction of 31 kcal/mol, suggesting that for small aldehydes the final dehydration reaction (and not the keto/enol tautomerization) may be the rate-determining step of the aldol reaction in zeolites. The study of Liu et al. provides important computational data for benchmarking the delta-cluster convergence of aldol reaction barriers, especially considering that the acetaldehyde self-aldol product (crotonaldehyde) and the acetone–formaldehyde aldol product (methyl vinyl ketone) are close structural isomers, allowing direct comparisons between the two aldol pathways.

It remains to be seen whether aldol reactions with larger aldehydes such as furfural and HMF in zeolites are also rate-limited by dehydration. It is conceivable that the bimolecular combination step could become rate-determining for the coupling of an enol with a large aldehyde such as HMF in the relatively confining space of HZSM-5. Furthermore, it is unclear whether the final dehydration step generally occurs via concerted or stepwise mechanisms[15] for different aldehyde coupling products (see Figure 4). We address these questions using quantum calculations on optimally confining delta clusters of HZSM-5.

Below, we report our results on delta-cluster convergence of free energies of intermediates and transition states for acetone aldol condensation with formaldehyde, furfural, and HMF, considering both concerted and stepwise processes where relevant. To organize all this information into predictions testable by experiments, we perform microkinetic calculations[16−18] to produce overall apparent activation energies for each process considered. In the end, we find that the neighbor-list radius of 4 Å is sufficient to converge barriers with respect to delta-cluster size for all reaction steps considered, yielding results in agreement with periodic DFT for a fraction of the computational cost. We predict that furfural and HMF exhibit faster aldol reactivity than does formaldehyde as controlled by different rate-determining steps because of charge delocalization from furan rings in furfural and HMF.

The remainder of this article is organized as follows: in Section 2 we describe the methods for constructing clusters, computing energies, locating transition states, and performing microkinetic calculations; in Section 3 we discuss our results for uncatalyzed reactions, cluster convergence of barriers, and aldol pathways for acetone with the panel of aldehydes; and in Section 4 we summarize and offer concluding remarks about future studies.

2. METHODS

2.1. Reaction Processes. To investigate the convergence of reaction barriers from clusters of HZSM-5, we studied all three steps of the aldol reaction between acetone and formaldehyde: (i) keto/enol tautomerization of acetone (Figure 5a), (ii) bimolecular combination between the acetone enol and formaldehyde (Figure 5b), and (iii) dehydration of the corresponding aldol product (also Figure 5b). Given these convergence results, we then modeled the bimolecular combinations between the acetone enol and the aldehydes—furfural and HMF (Figure 5c,d, respectively)—as well as their dehydrations (also in Figure 5c,d, respectively) in clusters of HZSM-5.

2.2. Zeolite Delta Clusters. Here we give a description of the delta-cluster method[5] as applied, for the first time, to computing reaction barriers. The delta-cluster approach is based on including all zeolite atoms that fall within the union of several spheres—all with the same radius (δ)—but centered at the following points: the zeolite Brønsted site oxygen atoms, and each atom of one or more relevant guest-molecule configurations, ensuring that the delta cluster is sufficient for enveloping the chemical transformations of the guest(s) under study. We note that applying the delta-cluster method using several different radii on the active atoms might produce even smaller clusters, but we favor the simplicity of using a single length scale to define delta clusters. For modeling reactions in zeolites, we have found it the most convenient to use estimates of both reactant and product guest configurations simultaneously to build delta clusters, ensuring that the resulting cluster is sufficient to envelop and confine the entire reaction path. Although the delta clusters studied here are significantly smaller than the HZSM-5 unit cell, the delta approach yields clusters that accurately account for confinement by including all relevant framework atoms needed to describe the physical chemistry and encompass the reactant system within the zeolite pore.

Because the delta-cluster method requires a priori estimates of guest-molecule coordinates, previous knowledge and/or lower-level methods can be useful for estimating guest-molecule locations. Our investigations indicate that the precise nature of a given delta cluster—e.g., its size and boundary

DOI: 10.1021/acs.jpcc.8b08684
J. Phys. Chem. C 2018, 122, 23230−23241

surface—is not overly sensitive to the accuracy of estimated guest configurations; these are required to indicate the broad region of intracrystalline zeolite space needed to treat a given reaction. In the current work, initial reactant and product geometries for acetone keto/enol tautomerization, and for bimolecular combination with formaldehyde, were taken from optimized clusters in our earlier studies of HZSM-5.[4] For the bimolecular combination of the enol with furfural, a new estimate of reactant/product geometries was obtained by converting a hydrogen on formaldehyde to a furan ring and reoptimizing reactants and products in a large cluster (δ = 7 Å) at PM6.[19] The same approach was used to generate clusters for enol−HMF, converting a hydrogen in furfural to a hydroxymethyl group. Clusters for the three water elimination reactions, which required estimates of water-binding geometries in HZSM-5, were found to be relatively insensitive to the precise location of water in the pore. The delta-cluster approach has been implemented in Schrödinger's Maestro[20] graphical user interface via a Python script, which is freely available from the authors or from Schrödinger.

As in our previous work,[4,21,22] the Brønsted acid site in HZSM-5 was chosen to be between Si(2) and Si(8), centered on O(13) (see Figure 6). Due to its proximity to the HZSM-5

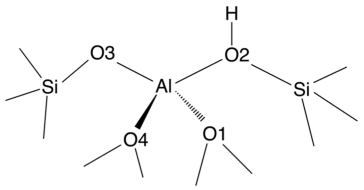

Figure 6. Two-dimensional representation of the Brønsted acid site in HZSM-5. We denote the active-site oxygens as O1, O2, O3, and O4 for simplicity; these are not the crystallographically sanctioned labels in HZSM-5, in which the oxygen labeled O2 corresponds to O(13).

channel intersection, O(13) is deemed a catalytically relevant site.[21] We note in Figure 6 that the active-site oxygen, O(13), is denoted O2 for ease of numbering (not the crystallographically sanctioned labels). Delta clusters were carved out from the periodic crystal and terminated at either Si or O atoms.[23] Hydrogen atoms were used to cap terminal Si or O atoms, with Si−H/O−H bond lengths set to 1.4/0.9 Å, respectively. In all calculations, terminal −H and −OH groups were frozen in their crystallographic positions. Fixing the oxygens of terminal −OH groups is important for freezing terminal OH wagging motions that can complicate convergence of optimizations and transition-state searches in finite zeolite clusters.

Generating consistent energetics for each multistep reaction pathway requires using a single, master cluster for keto/enol, combination, and dehydration reactions. This is trivial for periodic calculations, which use the same unit cell for each calculation. In contrast, the delta-cluster approach generates distinct, tailored clusters for each of these elementary steps. To generate a master delta cluster, we simply take the union of the elementary-step delta clusters and recompute all reactant, product, intermediate, and transition state energies and frequencies using geometries obtained from the smaller, tailored delta clusters. In principle, the master cluster could be different for acetone reacting with formaldehyde, furfural, or HMF. For simplicity, we used the master cluster for acetone−HMF for all three pathways. Overall, this computational process was found to be straightforward and efficient, involving a 38T master delta cluster that is roughly one-third the size of the HZSM-5 unit cell, and CPU times are roughly 20 times less than those using the entire unit cell in head-to-head comparisons running Vienna ab initio simulation package (VASP) on a single processor (see Table S1 in the Supporting Information (SI) for CPU times).

2.3. Computational Details. The B3LYP[24] hybrid density functional was used with the 6-311G(d,p)[25] basis set as implemented in Gaussian (version EM64L-G09RevB.01).[26] Dispersion corrections via the Grimme[27] approach (henceforth denoted B3LYP+D3) were made using the electronic structure program Jaguar[28] because the D3 option is not available in Gaussian09 (version EM64L-G09RevB.01). This approach[4] yielded a barrier for the keto/enol tautomerization of acetone in HZSM-5, in quantitative agreement with the cluster calculations of Boekfa et al.[14] using M06-2X/6-311+G(2df,2p) and with the periodic planewave calculations of Liu et al.[3] using the PBE density functional. To test the sensitivity of our computed barriers to changes in basis set and density functional, we computed acetone keto/enol barriers using either B3LYP+D3 or the dispersion-corrected wB97XD functional,[27] along with either 6-311G(d,p) or 6-311++G-(3df,3pd) basis sets. Figure S1 in the Supporting Information shows that all four approaches show similar cluster size convergence trends, with B3LYP+D3/6-311G(d,p) and wB97XD/6-311++G(3df,3pd) results consistently within 1 kcal/mol. Table S1 shows the CPU times corresponding to these calculations, indicating that B3LYP+D3/6-311G(d,p) is more than 40 times faster than wB97XD/6-311++G(3df,3pd), a speedup mostly from the difference in basis set size, from 1352 to 2957 basis functions, as shown in Table S1 (for a delta cluster with δ = 4.5 Å). To balance computational efficiency and accuracy, we apply the B3LYP+D3/6-311G(d,p) approach for the remaining work presented here.

Unless otherwise specified, all energies reported are Gibbs free energies in kcal/mol. Atomic charges for analyzing electronic structures of intermediates and transition states were calculated using the Merz−Kollman procedure to reproduce the electrostatic potential (ESP).[29,30] To obtain thermodynamic properties of reactants, products, intermediates, and transition states, we applied corrections for zero-point energy, nonzero temperature (to obtain internal energies), work (to obtain enthalpies), and entropy (to obtain Gibbs free energies) within the harmonic oscillator model (see the Supporting Information Table S2 for these corrections). In general, these corrections were not found to alter the trends obtained directly from the potential energies.

2.4. Locating Transition States. Here we briefly describe our procedure for locating transition states in this work (Supporting Information SI 4 describes additional details). Although we have located transition states for the keto/enol tautomerization and enol−formaldehyde combination in our earlier work,[4] we chose to ignore that information in this work, instead aiming to establish naïve convergence of these barriers (along with the barrier(s) for 3-oxobutanol dehydration) with respect to delta-cluster size. We find that a δ value of 4.0 Å is sufficient to converge these transition states; we subsequently applied this finding to the location of enol−furfural and enol−HMF combinations and aldol dehydration transition states.

All transition states were located using the Berny optimization algorithm,[31] confirmed as first-order saddle points by normal-mode analysis, and by steepest-descent calculations

DOI: 10.1021/acs.jpcc.8b08684
J. Phys. Chem. C 2018, 122, 23230−23241

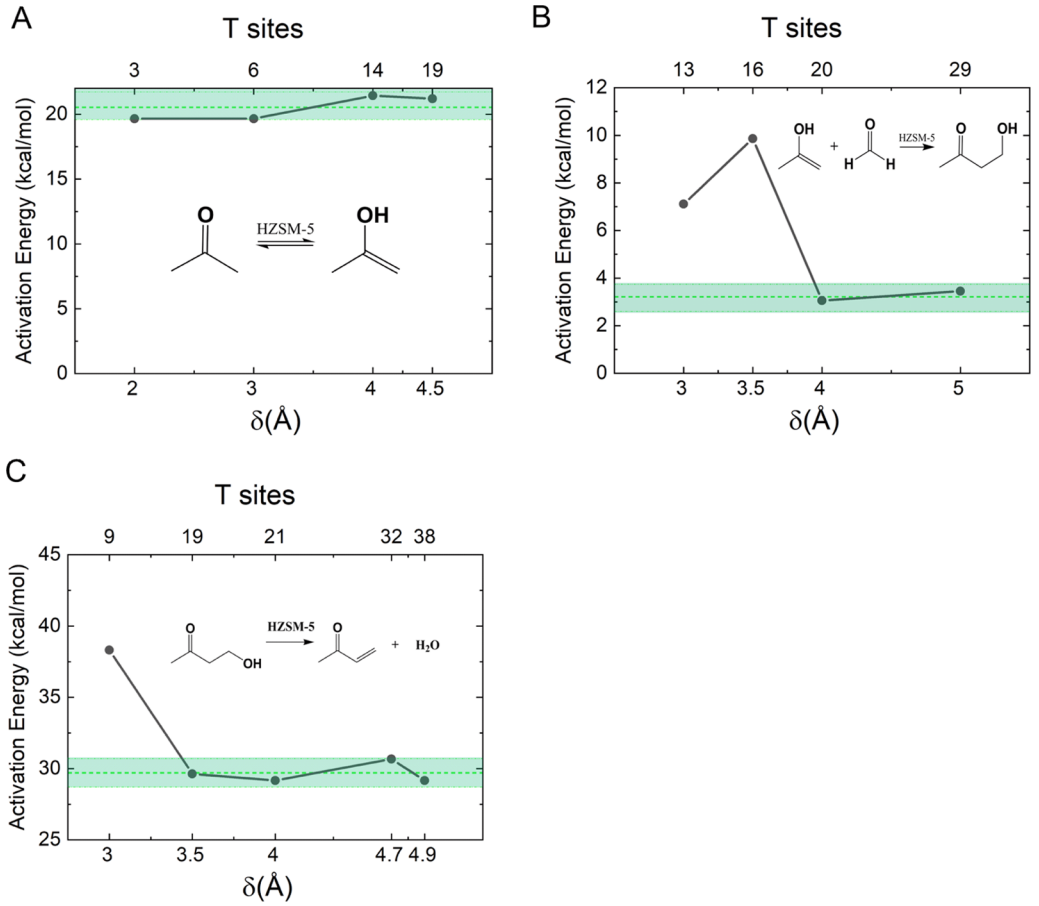

Figure 7. Convergence of bare electronic barriers for (A) keto/enol, (B) enol−formaldehyde combination, and (C) dehydration reactions, with various delta clusters of HZSM-5—each showing convergence with respect to system size to within ±1 kcal/mol (convergence band shaded in green).

to confirm that transition states connect with the desired reactant and product minima. Initial conditions for transition-state searches for the three acetone−formaldehyde reaction steps were obtained by bootstrapping: first finding transition states in smaller systems with respect to cluster size and level of theory and using those results as initial conditions to work up to the final transition-state calculations at B3LYP+D3 on converged delta clusters. Initial conditions for transition-state searches for acetone−furfural reaction steps were obtained by bootstrapping from acetone−formaldehyde transition states by transforming a hydrogen in formaldehyde to a furan ring and recomputing transition states—first at lower levels of theory and eventually at B3LYP+D3. Similarly, initial conditions for transition-state searches for acetone−HMF were obtained by bootstrapping from acetone−furfural transition states by transforming a hydrogen in furan to a hydroxymethyl group and recomputing transition states. Further details behind this approach can be found in SI 4.

2.5. Microkinetics Calculations. Microkinetic calculations are useful for generating testable predictions from complex, multistep reaction models.[16−18] For each reaction pathway, we seek to determine the apparent activation energy consistent with the temperature-dependent Gibbs free energies computed for reactants, products, intermediates, and transition states. As in our previous work,[18] we invoke the pseudo-steady-state approximation,[16,32] assuming that the concentrations of stable adsorbates are constant in time to yield a well-defined kinetic system that does not require information from the adsorption isotherms of reactants/products. Each aldol pathway consists of three or four elementary steps, assuming concerted or stepwise dehydration, respectively (see eqs 1 and 2). In eqs 1 and 2 below, "Z" is the HZSM-5 zeolite and "···" indicates a host−guest attraction. As detailed in SI 3, we use transition-state theory and the Arrhenius equation to construct a first-order rate constant for each elementary step. We then solve the resulting first-order, ordinary differential equation using the backward differentiation formula[33] to obtain the initial rate of production of the adsorbed enone product. This initial rate is obtained for each pathway at 80, 100, and 120 °C using the temperature-dependent Gibbs free energies (see Figure S2), and an Arrhenius analysis of these initial rates yields the apparent activation energy for each pathway (see Figure S3).

$$\mathrm{Z{\cdots}ace} \underset{k_{-1}}{\overset{k_1}{\rightleftharpoons}} \mathrm{Z{\cdots}enol} + \mathrm{Z{\cdots}ald} \underset{k_{-2}}{\overset{k_2}{\rightleftharpoons}} \mathrm{Z{\cdots}aldol} \underset{k_{-3}}{\overset{k_3}{\rightleftharpoons}} \mathrm{Z{\cdots}enone} + \mathrm{Z{\cdots}H_2O} \quad (1)$$

$$\mathrm{Z{\cdots}ace} \underset{k_{-1}}{\overset{k_1}{\rightleftharpoons}} \mathrm{Z{\cdots}enol} + \mathrm{Z{\cdots}ald} \underset{k_{-2}}{\overset{k_2}{\rightleftharpoons}} \mathrm{Z{\cdots}aldol} \underset{k_{-3}}{\overset{k_3}{\rightleftharpoons}} \mathrm{Z{\cdots}int} \underset{k_{-4}}{\overset{k_4}{\rightleftharpoons}} \mathrm{Z{\cdots}enone} + \mathrm{Z{\cdots}H_2O} \quad (2)$$

DOI: 10.1021/acs.jpcc.8b08684
J. Phys. Chem. C 2018, 122, 23230−23241

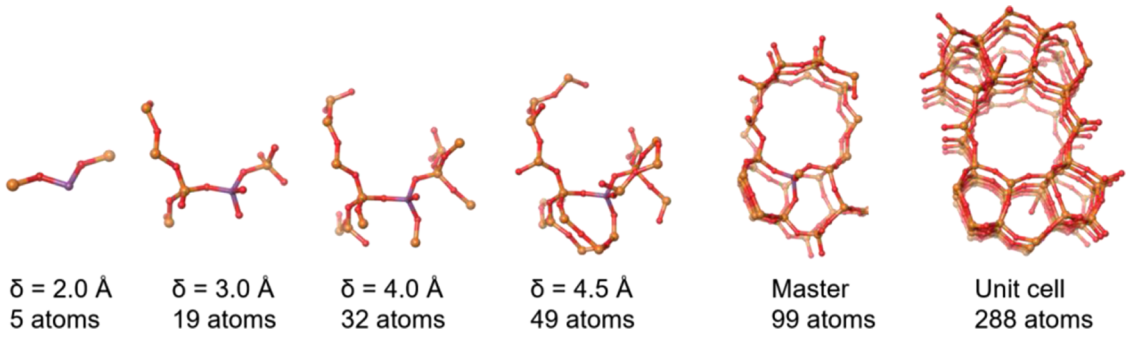

Figure 8. Various delta clusters shown along with the master delta cluster used for production calculations, and the HZSM-5 unit cell.

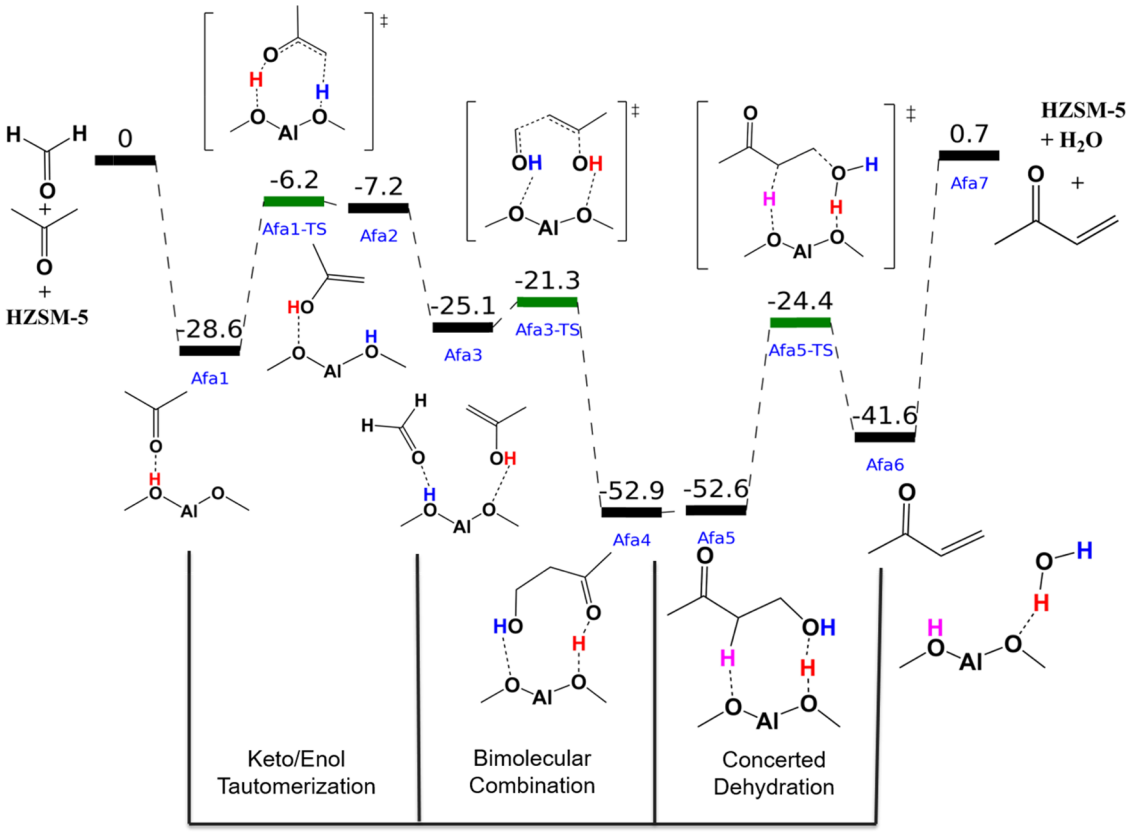

Figure 9. Energetics of reaction between acetone and formaldehyde in HZSM-5, assuming concerted dehydration. The calculated Gibbs free energies are in kcal/mol using B3LYP+D3/6-311G(d,p) with dispersion, zero-point energy, thermal, and entropic corrections. The hydrogen atoms involved in the reaction are highlighted with color. The dehydration barrier is 28.2 kcal/mol = 52.6 − 24.4 kcal/mol, and the apparent activation energy is 27.2 kcal/mol, indicating that dehydration is the rate-determining step of this overall process.

3. RESULTS AND DISCUSSION

Here we report our results in four parts for aldol reactions catalyzed by HZSM-5. Section 3.1 provides foundational results of two kinds: (i) gas-phase aldol energetics for all reaction systems to set baselines for quantifying catalytic activity (data in the Supporting Information); and (ii) calculation of acetone−formaldehyde barriers with respect to delta-cluster size to establish convergence. Section 3.2 describes the mechanisms and barriers for aldol condensation of acetone and formaldehyde in the master cluster of HZSM-5. Section 3.3 details mechanisms and barriers for acetone−furfural and acetone−HMF reactions, with a focus on how aldehyde size and structure influence the kinetics. In Section 3.4, we compare the various pathways by reporting the apparent activation energies obtained from microkinetics calculations and correlate these energies with microscopic barriers of rate-determining steps.

3.1. Foundations: Gas-Phase Energetics and Zeolite Cluster Convergence. Gas-phase energetics for all three reactions are shown in Figure S4. The magnitudes of these barriers indicate that keto/enol tautomerization is the rate-limiting step of the gas-phase process with a Gibbs free energy barrier of 65 kcal/mol, followed in magnitude by the dehydration step barriers in the range 53−58 kcal/mol. Below we report apparent activation energies for zeolite-catalyzed reactions in the range of 22−28 kcal/mol, indicating significant catalytic activity of the solid acid HZSM-5.

The convergence of activation energies with respect to delta-cluster size is shown for acetone keto/enol tautomerization (Figure 7A), enol bimolecular combination with formaldehyde

DOI: 10.1021/acs.jpcc.8b08684
J. Phys. Chem. C 2018, 122, 23230−23241

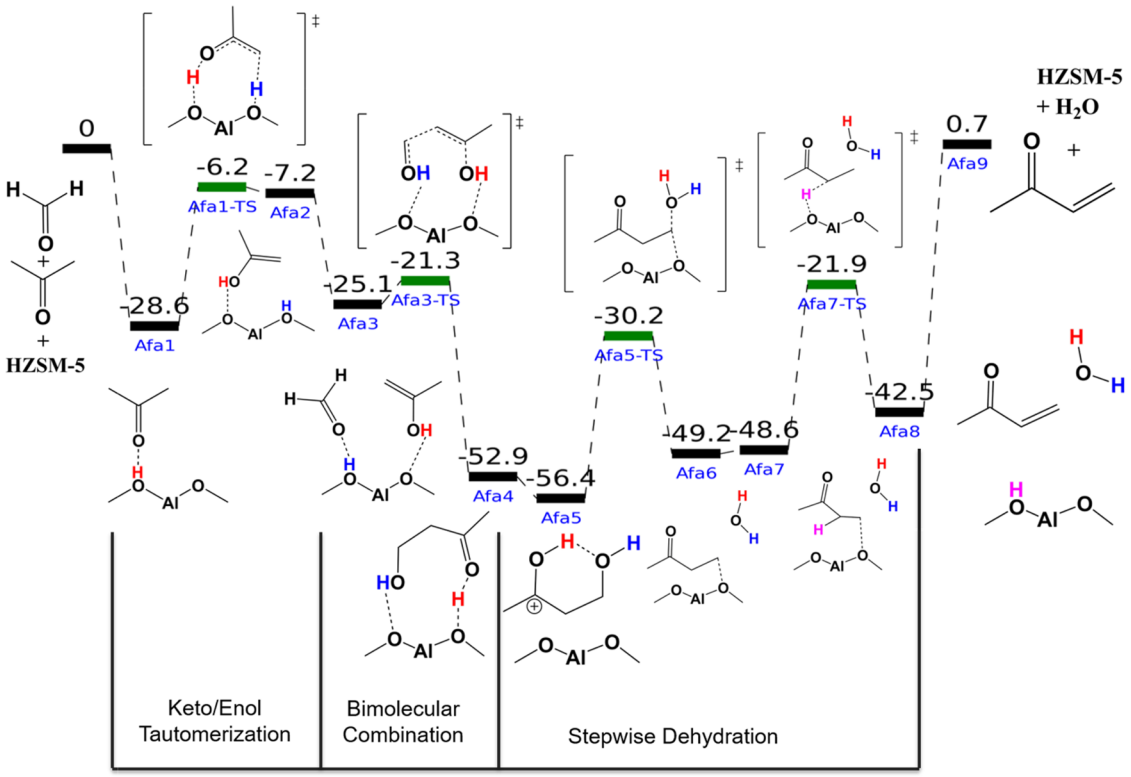

Figure 10. Energetics of reaction between acetone and formaldehyde in HZSM-5 via stepwise dehydration. The microkinetic apparent activation energy is 30.7 kcal/mol, while the composite stepwise dehydration barrier is 34.5 kcal/mol (Afa7-TS—Afa5). Comparison with the concerted energetics suggests that concerted dehydration is favored at ambient temperatures.

(Figure 7B), and 3-oxobutanol dehydration (Figure 7C)—all in delta clusters of HZSM-5. These results show that a single δ = 4.0 Å cutoff distance is sufficient to converge all three barriers to within 1 kcal/mol with respect to system size. We believe that 1 kcal/mol (i.e., "chemical accuracy") is the appropriate target for cluster convergence, as this target is balanced with targets for convergence with respect to basis set and level of theory. The converged delta-cluster sizes of 14T for keto/enol, 20T for bimolecular combination, and 21T for dehydration can be understood in terms of the guest chemistry involved. In particular, the keto/enol process involves the rearrangement of the small acetone molecule, requiring a relatively small surrounding cluster. The bimolecular combination cluster must envelope the larger enol−formaldehyde complex, requiring significantly more atoms. Finally, the dehydration cluster must allow for elimination of water, which has a small but nonzero effect on delta-cluster size. The single δ = 4.0 Å cutoff provides a convenient way to capture these effects and produces 34T/38T dehydration clusters for acetone−furfural/HMF. We have employed this 38T cluster as the master cluster for computing energetics for all microkinetics calculations reported below.

Figure 8 shows the master cluster, which contains 99 nonhydrogen atoms, in comparison with several smaller delta clusters and the ZSM-5 unit cell. Figure 8 shows how the master cluster treats confinement accurately while remaining a small fraction of the entire unit cell size.

3.2. Acetone−Formaldehyde Catalyzed by HZSM-5.

Figure 9 shows the reaction pathway for the acetone−formaldehyde aldol condensation in HZSM-5, with intermediates labeled as Afa1−7, transition states labeled as Afa1−5TS, and active hydrogens shown in color for emphasis. The initial step—keto/enol tautomerization (Afa1−2)—exhibits a Gibbs barrier of 22.4 kcal/mol, consistent with previous results.[3,4,14] As in our previous work,[4] Figure 9 shows a bimolecular combination step (Afa3−4) with a Gibbs barrier of 3.8 kcal/mol, characterized by a concerted rearrangement involving the simultaneous deprotonation of the Brønsted proton, carbon−carbon bond formation between the enol and formaldehyde, and reprotonation of the zeolite to regenerate a new Brønsted acid site.

Regarding the final major step of the process—aldol dehydration—as discussed above in the Introduction, both stepwise and concerted dehydration mechanisms may occur in zeolites,[15] analogous to E1 and E2 processes in homogenous media (see Figure 4). In their study of acetaldehyde self-aldol condensation (similar to the acetone−formaldehyde aldol reaction), Liu et al.[3] considered stepwise dehydration and found a rate-determining barrier of 30.9 kcal/mol. In the present work, we consider both stepwise and concerted dehydration mechanisms. Figure 9 shows the concerted dehydration (Afa5−6) with a Gibbs barrier of 28.2 kcal/mol, while Figure 10 shows a stepwise dehydration process (Afa5−8) with a composite Gibbs barrier of 34.5 kcal/mol computed from comparing Afa7-TS—Afa5 Gibbs energies. In this stepwise process, water loss occurs concurrently with the binding of a carbocation to a zeolite oxygen (Figure 10, Afa5-TS). [In another stepwise process (Figure S5 in SI) with an even higher barrier, water loss occurs later in the process.] Microkinetics calculations on the pathways in Figures 9 and 10 yield apparent activation energies of 27.2 kcal/mol (concerted) and 30.7 kcal/mol (stepwise)—the latter value being in close agreement with the results of Liu et al.[3] It is important to note that for a simple one-step process, the apparent activation

DOI: 10.1021/acs.jpcc.8b08684
J. Phys. Chem. C 2018, 122, 23230−23241

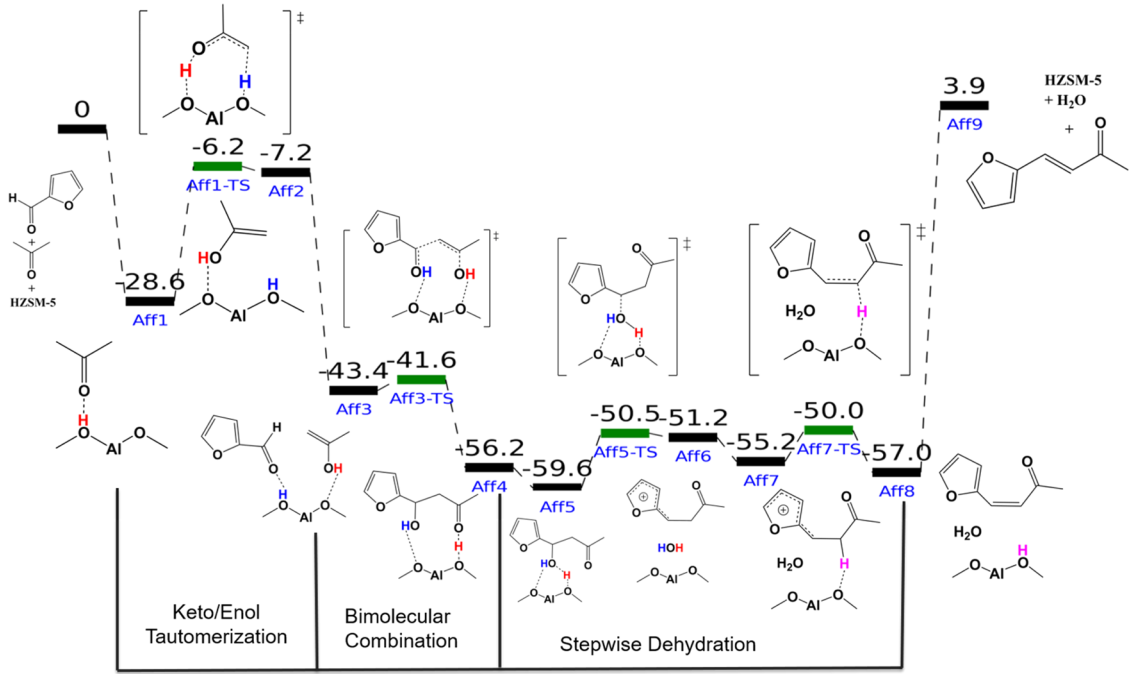

Figure 11. Energetics of reaction between acetone and furfural in HZSM-5 via stepwise dehydration, in which hydrogen transfer follows water loss. The microkinetic apparent activation energy is 24.3 kcal/mol, corresponding to the keto/enol tautomerization as the rate-determining step with a Gibbs barrier of 22.4 kcal/mol.

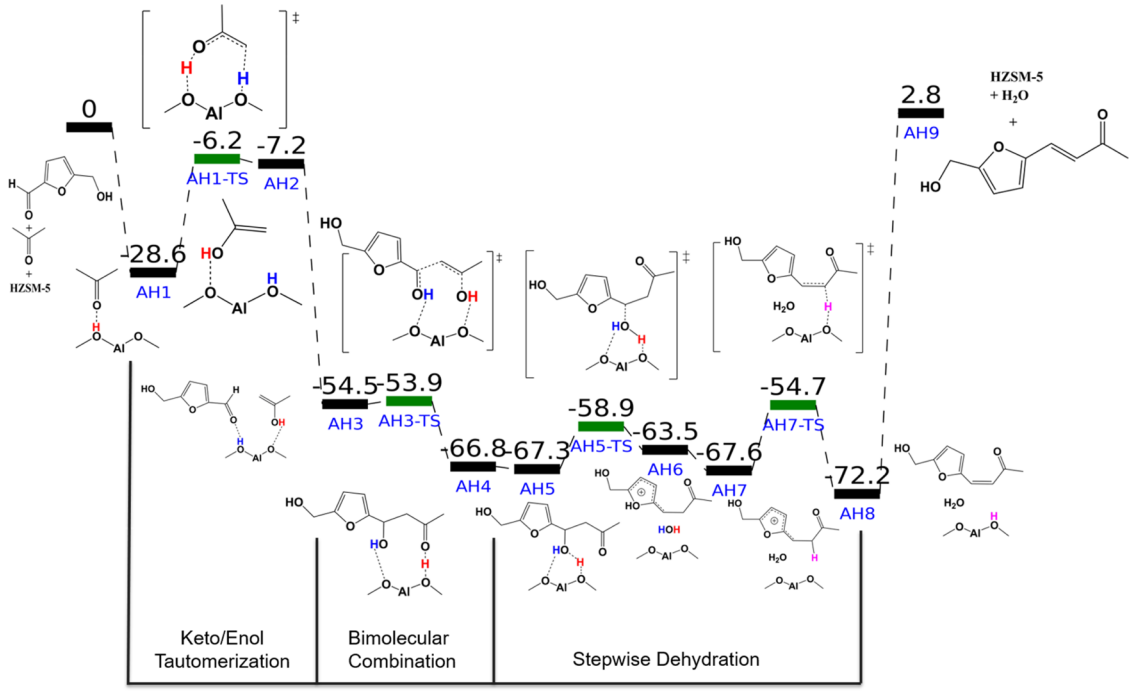

Figure 12. Energetics of reaction between acetone and HMF in HZSM-5 via stepwise dehydration, in which hydrogen transfer follows water loss. The microkinetic apparent activation energy is 21.5 kcal/mol, corresponding to the keto/enol tautomerization being the rate-determining step, whose Gibbs barrier is 22.4 kcal/mol.

energy corresponds to a microscopic enthalpic barrier, and not to the Gibbs barrier; as such, we do not expect a rate-limiting Gibbs barrier to exactly match a corresponding apparent activation energy. Overall, these results show that (i) converged clusters and periodic DFT calculations produce quantitative agreement, (ii) dehydration is the rate-determining step of acetone–formaldehyde aldol condensation in HZSM-5, and (iii) the concerted dehydration of the aldol product is favored over the stepwise dehydration in HZSM-5, especially at ambient temperatures. This last conclusion may extend to other aldol reactions of small molecules such as acetaldehyde self-aldol condensation; however, it remains unclear how aldol products involving larger molecules like furfural and HMF eliminate water, which we explore below.

DOI: 10.1021/acs.jpcc.8b08684
J. Phys. Chem. C 2018, 122, 23230–23241

3.3. Acetone−Furfural/Acetone−HMF Catalyzed by HZSM-5. Figures 11 and 12 show the Gibbs energy profiles for the aldol condensations of acetone−furfural and acetone−HMF, respectively, computed in the 38T master delta cluster of HZSM-5. We consider these larger, biomass-derived aldehydes to investigate whether significantly increasing aldehyde size changes the energetics and mechanisms of aldol condensation. Simple geometrical estimates may serve as a useful guide. According to the Database of Zeolite Structures,[34] the maximum diameter of a sphere that can diffuse through HZSM-5 channels is 4.5−4.7 Å, while that of the channel intersection is roughly 6.4 Å. In comparison, an effective diameter of HMF is roughly 5.9−6.2 Å, as estimated from a combination of molecular structure and thermodynamic critical properties.[10] These estimates suggest that while diffusion of HMF through HZSM-5 should be sluggish, HMF may experience some orientation freedom in the HZSM-5 channel intersection. The question remains whether there is sufficient freedom for facile aldol coupling. The data in Figures 11 and 12 indicate, perhaps surprisingly, that there is plenty of room in the HZSM-5 channel intersection. Indeed, steps Aff3−4 in Figure 11 for acetone−furfural and AH3−4 in Figure 12 for acetone−HMF give bimolecular Gibbs barriers of 1.8 and 0.6 kcal/mol, respectively, indicating that these aldol combination processes are even more facile in the HZSM-5 channel intersection than for acetone−formaldehyde (3.8 kcal/mol) and are comparable to that for acetaldehyde self-condensation (1.4 kcal/mol).[3] These results provide a clear example of the utility of simple geometrical estimates.

The concerted dehydration of the acetone−formaldehyde aldol product shown in Figure 9 requires an isoenergetic realignment of the aldol product (Figure 9, Afa4−5), pointing the newly made OH group toward the regenerated zeolite Brønsted acid site to form the H_2O leaving group. Our calculations on the acetone−furfural and acetone−HMF aldol products suggest that such a realignment is not possible for these bulkier species given the available pore space in HZSM-5. Instead, stepwise dehydration pathways are considered in Figures 11 and 12 involving early loss of water and subsequent carbocation formation (Figure 11, Aff6; Figure 12, AH6). [Alternative stepwise mechanisms for acetone−furfural and acetone−HMF dehydration with later loss of water are shown in the Supporting Information Figures S6 and S7, respectively, showing much higher composite dehydration barriers (32.8 and 25.2 kcal/mol, respectively).]

The remarkably flat Gibbs energy landscapes for the stepwise dehydrations in Figures 11 and 12, as compared to that in Figure 10, suggest that the furfural and HMF aldol products possess mechanisms for stabilizing these dehydration intermediates and transition states. We hypothesize that the carbocations in Figures 11 and 12 are stabilized by electron donation from furan rings, implied by the resonance structures shown in Figure 13. To test this hypothesis, we computed ESP charges of key species involved in these stepwise dehydrations (Table 1), which reveal several features of the dehydration

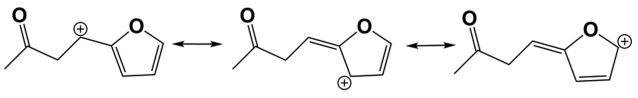

Figure 13. Resonance stabilization of the carbocation formed at Aff6 in Figure 10.

Table 1. ESP Charges of Key Dehydration Species from Figures 9−11[a]

structure name	species	formaldehyde Figure 9	furfural Figure 10	HMF Figure 11
A5	aldol + Hz	0.74 (Afa5)	0.85 (Aff5)	0.66 (AH5)
	furan ring		0.29 (Aff5)	0.29 (AH5)
A6	aldol + Hz − H_2O	0.01 (Afa6)	0.99 (Aff6)	0.94 (AH6)
	furan ring		0.65 (Aff6)	0.55 (AH6)

[a]These charges include all the aldol atoms (aldol) plus the zeolite hydrogen (red Hz). Upon dehydration (A6), the total charge deducts the charge of water (H_2O).

mechanisms. First, these charges establish that for structures "A5"—Afa5 for formaldehyde in Figure 10, Aff5 for furfural in Figure 11, and AH5 for HMF in Figure 12—the aldol products are substantially protonated with composite ESP charges in the range 0.66−0.85|e|. In this way, the three systems are similar; in the next step (A6), however, they differ substantially. Table 1 shows that the formaldehyde aldol structure Afa6 has a vanishing composite charge, balanced by a covalent alkoxy linkage to a zeolite oxygen, while structures Aff6 (furfural) and AH6 (HMF) exhibit near-unit positive charges (0.94−0.99|e|). Table 1 further shows that most of the positive charges in Aff6 and AH6 are delocalized into the furan rings consistent with the resonance structures in Figure 13 and that this represents a buildup of furanic positive charge relative to those in Aff5 and AH5. The resulting composite dehydration Gibbs barriers are 9.1 and 12.9 kcal/mol, respectively, for acetone−furfural and acetone−HMF. These low dehydration barriers make the keto/enol tautomerization the rate-determining step for both acetone−furfural and acetone−HMF aldol reactions.

3.4. Microkinetics-Calculated Apparent Activation Energies. Table 2 summarizes the findings of our work, showing that acetone−formaldehyde aldol condensation is predicted to be rate-limited by concerted dehydration, while acetone−furfural/HMF aldol condensations are predicted to be rate-limited by the keto/enol tautomerization. Our results suggest the somewhat surprising prediction that the bulkier aldehydes engage in faster aldol chemistry because of the availability of the furan ring to donate electrons to stabilize the carbocation formed in stepwise dehydration. This is both interesting scientifically and important technologically due to the relevance of HMF as a biomass-derived platform chemical.

We note that Liu et al. predicted a low-barrier (11.5 kcal/mol)[3] mechanism for the cross-coupling between acetaldehyde and furan without keto/enol tautomerization. The process studied by Liu et al. cleverly exploits the fact that the alpha carbon in furan is intrinsically nucleophilic and thus may not require catalytic activation. It is interesting to explore whether a similar mechanism can also be efficient for acetone−furfural coupling. We applied the delta-cluster methods described above to address this question, considering furfural bound to the Brønsted site attacked by acetone (shown in the Supporting Information Figure S8), finding a bimolecular combination Gibbs barrier of 60.7 kcal/mol, suggesting that the alpha carbon of acetone remains too unreactive without Brønsted acid activation. As such, we predict that the bold apparent activation energies shown in Table 2 are the correct

DOI: 10.1021/acs.jpcc.8b08684
J. Phys. Chem. C 2018, 122, 23230−23241

Table 2. Summary of Findings for Each Reaction/Dehydration Mechanism, Listing the Apparent Activation and the Corresponding Rate-Determining Step and Microscopic Gibbs Barrier[a]

aldehyde name	dehydration mechanism	microkinetic apparent activation energies (kcal/mol)	rate-determining step	microscopic barrier of rate-determining step (kcal/mol)
formaldehyde	concerted	**27.2**[b]	III	**28.2**
	stepwise 1 (water loss/H transfer)	30.7	III	34.5
	stepwise 2 (H transfer/water loss)	41.8	III	45.4
furfural	stepwise 1 (water loss/H transfer)	**24.3**	I	**22.4**
	stepwise 2 (H transfer/water loss)	34.0	III	32.8
HMF	stepwise 1 (water loss/H transfer)	**21.5**	I	**22.4**
	stepwise 2 (H transfer/water loss)	25.2	III	26.6

[a]Steps labeled as: (I) keto/enol tautomerization, (II) bimolecular combination, and (III) dehydration. [b]Numbers in bold indicate rate-determining steps.

activation energies for these reactions, assuming that catalysis occurs at O(13) in HZSM-5.

4. SUMMARY AND CONCLUDING REMARKS

We have performed DFT calculations to investigate the convergence of reaction barriers with respect to zeolite cluster size for aldol reactions catalyzed in HZSM-5 zeolite. In particular, we have tested the convergence properties of the delta-cluster approach, which systematically treats zeolite confinement using a single neighbor-list radius (δ). We have studied the aldol reactions between acetone and formaldehyde, furfural, and hydroxymethyl-furfural (HMF)—systems relevant to biomass conversion—as important platforms for establishing convergence of delta-cluster treatments of zeolite confinement and for investigating how changing aldehyde size may influence energetics and mechanisms of aldol condensation.

Regarding cluster convergence, we had shown in a previous publication that with a single convergence parameter, the delta-cluster approach can produce optimally tailored clusters for computing thermodynamic reaction energies for a range of different reactions in zeolites at a relatively small computational cost as compared with other approaches. In the present work, we examined whether a single convergence parameter may also allow for converging barriers in zeolites for a range of different reactions. We found above that with a single length scale of δ = 4.0 Å, the delta-cluster approach generated tailored clusters of size up to 38T, where T = Si or Al tetrahedral atoms, for computing barriers that are converged with respect to system size within 1 kcal/mol. We found quantitative agreement with comparable periodic planewave DFT calculations, but with a speedup from using optimized delta clusters of a factor of almost 20 when compared with VASP calculations on a single processor. As such, the delta-cluster method presents an attractive alternative to periodic calculations in that it produces cluster models of zeolites in which energies are convergent and confinement effects are accounted for at significantly smaller system sizes (99 framework atoms) compared to periodic calculations that use the entire unit cell (288 framework atoms). The delta-cluster approach may also be applicable to modeling host/guest chemistry in metal−organic frameworks, polymer matrices, and other nanoporous environments.

Regarding aldol condensation, we have modeled the acid-catalyzed reaction in HZSM-5 in three steps: keto/enol tautomerization of acetone, bimolecular combination between each aldehyde and the enol, and aldol dehydration. Our calculations predict that aldol dehydration in HZSM-5 is concerted for the formaldehyde product; however, the process is stepwise for furfural and HMF because they are too bulky to realign for the concerted process, and the furan ring donates electron density to stabilize carbocations that form in the stepwise process. The apparent activation energies computed from microkinetics calculations actually anticorrelate with aldehyde size: 27.2 kcal/mol for acetone−formaldehyde (controlled by dehydration), 24.3 kcal/mol for acetone−furfural (limited by keto/enol tautomerization), and 21.5 for acetone−HMF (limited also by keto/enol). These results suggest that the bulkier, furan-containing aldehydes exhibit faster aldol reactivity because of electron delocalization from their furan rings. Future work will involve examining how this reactivity may yield coke in zeolites and how such coke-forming mechanisms can be tuned by changing zeolite pore size.

■ ASSOCIATED CONTENT

Supporting Information

The Supporting Information is available free of charge on the ACS Publications website at DOI: 10.1021/acs.jpcc.8b08684.

Barrier convergence of functional and basis set; thermodynamic energy correction; microkinetic calculation; locating transition states; gas phase, uncatalyzed aldol condensations; acetone−formaldehyde/furfural/HMF catalyzed by HZSM-5 via stepwise dehydration pathways; structures of species on the energetic profiles: optimized structures (reactant, transition state, product) for keto/enol tautomerization, enol−formaldehyde/furfural/HMF combination and aldol dehydration (concerted/stepwise) reactions in delta clusters of HZSM-5 (PDF)

■ AUTHOR INFORMATION

Corresponding Author

*E-mail: auerbach@chem.umass.edu. Tel: +1-413-545-1240.

ORCID

Woody Sherman: 0000-0001-9079-1376

Scott M. Auerbach: 0000-0001-8598-3082

Author Contributions

#A.N.M. and Q.S. contributed equally to this work.

Notes

The authors declare no competing financial interest.

■ ACKNOWLEDGMENTS

We acknowledge generous funding from the NSF under award CBET-1512442.

DOI: 10.1021/acs.jpcc.8b08684
J. Phys. Chem. C 2018, 122, 23230−23241

REFERENCES

(1) Jacobs, P.; Flanigen, E. M.; Jansen, J.; van Bekkum, H. *Introduction to Zeolite Science and Practice*; Elsevier: NY, 2001.

(2) Auerbach, S. M.; Carrado, K. A.; Dutta, P. K. *Handbook of Zeolite Science and Technology*; CRC Press: Boca Raton, 2003.

(3) Liu, C.; Evans, T. J.; Cheng, L.; Nimlos, M. R.; Mukarakate, C.; Robichaud, D. J.; Assary, R. S.; Curtiss, L. A. Catalytic Upgrading of Biomass-Derived Compounds via C−C Coupling Reactions: Computational and Experimental Studies of Acetaldehyde and Furan Reactions in HZSM-5. *J. Phys. Chem. C* **2015**, *119*, 24025−24035.

(4) Migues, A. N.; Vaitheeswaran, S.; Auerbach, S. M. Density Functional Theory Study of Mixed Aldol Condensation Catalyzed by Acidic Zeolites HZSM-5 and HY. *J. Phys. Chem. C* **2014**, *118*, 20283−20290.

(5) Migues, A. N.; Muskat, A.; Auerbach, S. M.; Sherman, W.; Vaitheeswaran, S. On the Rational Design of Zeolite Clusters. *ACS Catal.* **2015**, *5*, 2859−2865.

(6) Tuma, C.; Sauer, J. Treating Dispersion Effects in Extended Systems by Hybrid MP2:DFT Calculations - Protonation of Isobutene in Zeolite Ferrierite. *Phys. Chem. Chem. Phys.* **2006**, *8*, 3955−3965.

(7) West, R. M.; Liu, Z. Y.; Peter, M.; Gärtner, C. A.; Dumesic, J. A. Carbon−Carbon Bond Formation for Biomass-Derived Furfurals and Ketones by Aldol Condensation in a Biphasic System. *J. Mol. Catal. A: Chem.* **2008**, *296*, 18−27.

(8) Climent, M. J.; Corma, A.; Iborra, S. Conversion of Biomass Platform Molecules into Fuel Additives and Liquid Hydrocarbon Fuels. *Green Chem.* **2014**, *16*, 516−547.

(9) Kikhtyanin, O.; Bulánek, R.; Frolich, K.; Čejka, J.; Kubička, D. Aldol Condensation of Furfural with Acetone over Ion-Exchanged and Impregnated Potassium Bea Zeolites. *J. Mol. Catal. A: Chem.* **2016**, *424*, 358−368.

(10) Jae, J.; Tompsett, G. A.; Foster, A. J.; Hammond, K. D.; Auerbach, S. M.; Lobo, R. F.; Huber, G. W. Investigation into the Shape Selectivity of Zeolite Catalysts for Biomass Conversion. *J. Catal.* **2011**, *279*, 257−268.

(11) Shen, W.; Tompsett, G. A.; Hammond, K. D.; Xing, R.; Dogan, F.; Grey, C. P.; Conner, W. C. J.; Auerbach, S. M.; Huber, G. W. Liquid Phase Aldol Condensation Reactions with $MgO-ZrO_2$ and Shape-Selective Nitrogen-Substituted NaY. *Appl. Catal., A* **2011**, *392*, 57−68.

(12) Tabasso, S.; Cravotto, G. Platform Chemicals from Biomass Using Microwave Irradiation. In *Production of Biofuels and Chemicals with Microwave*; Fang, Z., Smith, J. R. L., Qi, X., Eds.; Springer Science + Business Media: Dordrecht, 2015.

(13) Solans-Monfort, X.; Bertran, J.; Branchadell, V.; Sodupe, M. J. Keto-Enol Isomerization of Acetaldehyde in HZSM5. A Theoretical Study Using the ONIOM2 Method. *J. Phys. Chem. B* **2002**, *106*, 10220−10226.

(14) Boekfa, B.; Pantu, P.; Probst, M.; Limtrakul, L. Adsorption and Tautomerization Reaction of Acetone on Acidic Zeolites: The Confinement Effect in Different Types of Zeolites. *J. Phys. Chem. C.* **2010**, *114*, 15061−15067.

(15) Kim, S.; Robichaud, D. J.; Beckham, G. T.; Paton, R. S.; Nimlos, M. R. Ethanol Dehydration in HZSM-5 Studied by Density Functional Theory: Evidence for a Concerted Process. *J. Phys. Chem. A.* **2015**, *119*, 3604−3614.

(16) Dumesic, J. A. *Microkinetics of Heterogeneous Catalysis*; American Chemical Society: Washington, 1993.

(17) Xu, Y.; Lausche, A. C.; Wang, S.; Khan, T. S.; Abild-Pedersen, F.; Studt, F.; Nørskov, J. K.; Bligaard, T. In Silico Search for Novel Methane Steam Reforming Catalysts. *New J. Phys.* **2013**, *15*, No. 125021.

(18) Agarwal, V.; Huber, G. W.; Conner, W. C., Jr.; Auerbach, S. M. Kinetic Stability of Nitrogen-Substituted Sites in HY and Silicalite from First Principles. *J. Catal.* **2010**, *270*, 249−255.

(19) Tubert-Brohman, I.; Guimarães, C. R. W.; Jorgensen, W. L. Extension of the PDDG/PM3 Semiempirical Molecular Orbital Method to Sulfur, Silicon, and Phosphorus. *J. Chem. Theory Comput.* **2005**, *1*, 817−823.

(20) Maestro. *Schrödinger Release 2018-1*; Schrödinger, LLC: NY, 2018.

(21) Agarwal, V.; Huber, G. W.; Conner, W. C., Jr.; Auerbach, S. M. DFT Study of Nitrided Zeolites: Mechanism of Nitrogen Substitution in HY and Silicalite. *J. Catal.* **2010**, *269*, 53−63.

(22) Vaitheeswaran, S.; Green, S. K.; Dauenhauer, P.; Auerbach, S. M. On the Way to Biofuels from Furan: Discriminating Diels−Alder and Ring-Opening Mechanisms. *ACS Catal.* **2013**, *3*, 2012−2019.

(23) van Koningsveld, H.; Jansen, J. C.; van Bekkum, H. The Monoclinic Framework Structure of Zeolite H-ZSM-5. Comparison with the Orthorhombic Framework of As-synthesized ZSM-5. *Zeolites* **1990**, *10*, 235−242.

(24) Becke, A. D. Density-functional Thermochemistry. III. The Role of Exact Exchange. *J. Chem. Phys.* **1993**, *98*, 5648−5652.

(25) Krishnan, R. B.; Binkley, J. S.; Seeger, R.; Pople, J. A. Self-Consistent Molecular Orbital Methods. XX. A Basis Set for Correlated Wavefunctions. *J. Chem. Phys.* **1980**, *72*, 650−654.

(26) Frisch, M. J.; et al. *Gaussian 09*, revision B.01, Gaussian, Inc.: Wallingford, CT, 2009.

(27) Grimme, S. Semiempirical GGA-type Density Functional Constructed with a Long-range Dispersion Correction. *J. Comput. Chem.* **2006**, *27*, 1787−1799.

(28) Bochevarov, A. D.; Harder, E.; Hughes, T. F.; Greenwood, J. R.; Braden, D. A.; Philipp, D. M.; Rinaldo, D.; Halls, M. D.; Zhang, J.; Friesner, R. A. Jaguar: A High-Performance Quantum Chemistry Software Program with Strengths in Life and Materials. *Int. J. Quantum Chem.* **2013**, *113*, 2110−2142.

(29) Singh, U. C.; Kollman, P. A. An Approach to Computing Electrostatic Charges for Molecules. *J. Comput. Chem.* **1984**, *5*, 129−145.

(30) Besler, B. H.; Merz, K. M., Jr.; Kollman, P. A. Atomic Charges Derived from Semiempirical Methods. *J. Comput. Chem.* **1990**, *11*, 431−439.

(31) Schlegel, H. B. Optimization of Equilibrium Geometries and Transition Structures. *J. Comput. Chem.* **1982**, *3*, 214−218.

(32) Gusmão, G. S.; Christopher, P. A General and Robust Approach for Defining and Solving Microkinetic Catalytic Systems. *AIChE J.* **2015**, *61*, 188−199.

(33) Brayton, R. K.; Gustavson, F. G.; Hachtel, G. D. A New Efficient Algorithm for Solving Differential-Algebraic Systems Using Implicit Backward Differentiation Formulas. *Proc. IEEE* **1972**, *60*, 98−108.

(34) Baerlocher, C.; McCusker, L. B.; Olson, D. H. *Atlas of Zeolite Framework Types*; Elsevier: NY, 2007.

DOI: 10.1021/acs.jpcc.8b08684
J. Phys. Chem. C 2018, 122, 23230−23241